

Alfvén Eigenmode stability with beams in ITER-like plasma¹

N. N. Gorelenkov 1), H. L. Berk 2), R. V. Budny 1)

1) Princeton Plasma Physics Laboratory, P.O. Box 451, Princeton, NJ, USA 08543-0451

2) IFS, Austin, Texas.

Toroidicity Alfvén Eigenmodes (TAE) in ITER can be driven unstable by two groups of energetic particles, the 3.5 MeV α -particle fusion products and the tangentially injected 1 MeV beam ions. Stability conditions are established using the perturbative NOVA/NOVA-K codes [1, 2]. A quasi-linear diffusion model is then used to assess the induced redistribution of energetic particles.

1 ITER plasma modeling

Equilibrium plasma profiles of an ITER nominal discharge are calculated by TRANSP code [3] and are presented in Fig. 1 plotted as functions of minor radius variable r/a . The plasma parameters are: the major plasma radius, $R_0 = 6.2\text{ m}$, the minor radius, $a = 2\text{ m}$, the deuterium negative NBI injection power at energy $E_{b0} = 1\text{ MeV}$, is $P_{NBI} = 33\text{ MW}$, the vacuum magnetic field on axis is $B_0 = 5\text{ T}$, the total central beta is $\beta_0 = 6.7\%$ and the central ion and electron temperatures are $T_{i0} = 19.5\text{ keV}$, and $T_{e0} = 23.5\text{ keV}$. TRANSP simulations used NBI applied tangentially $\Delta Z = 0.55\text{ m}$ below the magnetic axis in the baseline case. Three addition configurations have been studied with the same plasma beta: at $T_{i0} = 19.5\text{ keV}$ with on-axis and $\Delta Z = 0.35\text{ m}$ NBI; and at $T_{i0} = 25.3\text{ keV}$ on-axis NBI.

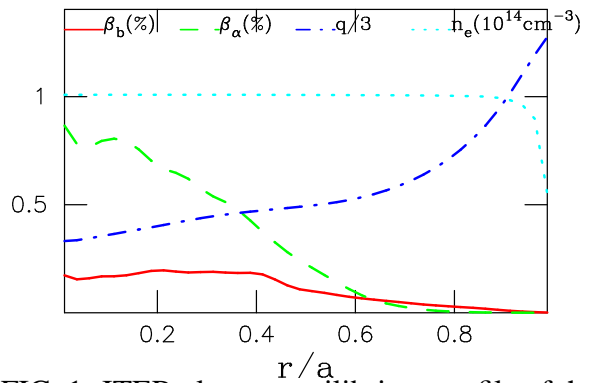


FIG. 1: ITER plasma equilibrium profile of the beam beta β_b , the fusion alphas beta β_α , the safety factor q , and the electron density n_e .

2 NBI ion anisotropic distribution function

If NBI generates a narrow pitch angle distribution it is modeled as follows. The distribution has the form,

$$f_b = \frac{f_\chi(\chi)}{v^3 + v_*^3} C(v, r), \text{ if } v < v_{b0}, \quad (1)$$

and $f_b = 0$ if $v > v_{b0}$, where $f_\chi(\chi, v, r) \equiv e^{-(\chi - \chi_0)^2 / \delta\chi^2}$, $\chi \equiv v_{||} / v$ is the taken in the equatorial plane at the low field side, $\delta\chi^2 \ll \chi_0^2$ is assumed. In this formula $\delta\chi$ is the width of the pitch angle distribution function, v_* is the conventional critical velocity, v_{b0} is the injection velocity, $C(v, r)$ is the normalization function. Ions injected in the passing region parallel to the current flow $\chi_0 > 0$, while the trapped and the counter-passing particles only arise due to Coulomb collisional scattering. The pitch angle width $\delta\chi(v, r)$ changes due to the Coulomb scattering [4, 5] with the diffusion coefficient given by $D_{\chi\chi} \simeq v_*^3 / v^3 \tau_{se}$. Simultaneously as the ions slow down due to velocity drag we find $v^3 = (v_*^3 + v_{b0}^3) e^{-3t/\tau_{se}} - v_*^3$, where τ_{se} is the ion slowing down time due to collisions with electrons. At a given v , for a particle injected at velocity v_{b0} . the pitch angle width is broadened according to $\delta\chi^2 = \delta\chi_0^2 + \int_0^t D_{\chi\chi} dt$, where $\delta\chi_0$ is the initial width due to ion finite orbit width (FOW) and plasma aspect ratio effects. Thus it follows that the width is given by

$$\delta\chi^2(v, r) = \delta\chi_0^2 - \frac{1}{3} \ln \left[\frac{v^3 (1 + v_*^3 / v_{b0}^3)}{v^3 + v_*^3} \right]. \quad (2)$$

¹This work supported by DoE contracts No. DE-AC02-76CH03073 and DE-FG03-96ER-54346

The center of the pitch angle Gaussian distribution function, χ_0 , is computed by taking the first moment of the numerical distribution function generated by TRANSP. In the case analyzed we obtained $\chi_0 \simeq 0.8$ near the region of interest. i.e. $r/a \simeq 0.5$ and χ_0 does not change significantly in the vicinity of the TAE location.

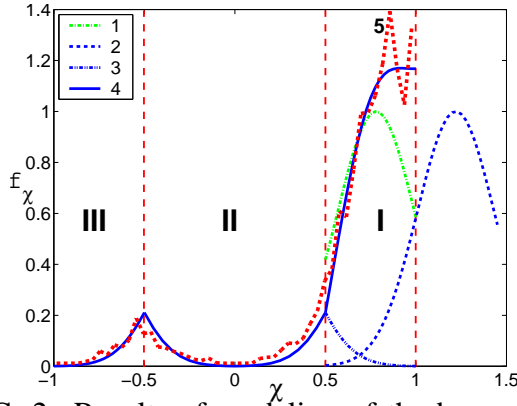


FIG. 2: Results of modeling of the beam ion pitch angle distribution function as given by Eq.(4) (curve 4) and its comparison with the TRANSP simulation (curve 5) for parameters $\delta\chi = 0.3$ and $r/R = 1/6$. Also shown are different terms for region I: curves 1 and 2 correspond to first and second terms in the right hand side of Eq.(3), whereas curve 3 is the absolute value of the sink term (second term of Eq.(4) for region I).

If the pitch angle width becomes large, the above χ dependence of the distribution function needs to be modified to account for particle scattering into different regions. Consider three regions: (I) co-passing with $\chi_{s+} < \chi < 1$, where χ_{s+} is the pitch angle at the separatrix between the co-passing and trapped ones; (II) trapped $\chi_{s-} < \chi < \chi_{s+}$; and (III) counter-passing $-1 < \chi < \chi_{s-}$, where χ_{s-} refers to the separatrix between the counter-passing and trapped regions. In the case of a large aspect ratio plasma $\chi_{s+} = -\chi_{s-} = \sqrt{2}\epsilon$. Particle conservation requires that the fluxes in and out the separatrix region are equal $f'(\chi_{s+} + \epsilon) = f'(\chi_{s-} - \epsilon) + 2f'(\chi_{s+} - \epsilon)$ with the trapped ion distribution function inside the region II even in χ .

Since the possible pitch angle range is bounded by $|\chi| < 1$, image particle sources can be introduced in order not to have diffusive fluxes at the boundaries. In that case the

distribution function satisfies the physical requirement of zero derivative at the boundary

$$f_{\chi p}(\chi) = \phi(\chi) \equiv e^{-(\chi-\chi_0)^2/\delta\chi^2} + e^{-(\chi-2+\chi_0)^2/\delta\chi^2}, \quad (3)$$

where two terms correspond in the right hand side correspond to curves 1 and 2 shown in Fig. 2. Since particles are diffusing out of the region I an image sink needs to be introduced. For the regions II and III image sources adequately represent the solution so that finally we obtain

$$f_{\chi} = \begin{cases} \phi(\chi) - \frac{1}{2}\phi(2\chi_{s+} - \chi), & \text{region I} \\ \frac{1}{2}\phi(-\chi) + \frac{1}{2}\phi(\chi), & \text{II} \\ \frac{1}{2}\phi(2\chi_{s+} + \chi), & \text{III} \end{cases}. \quad (4)$$

The procedure described is valid for a broad range of pitch angle widths and the truncation only becomes invalid at low velocity when it is necessary to account for collisional fluxes resulting from multiple reflections from the confinement boundaries. But in our analysis fast ions at energies such that $\delta\chi > 1$, are typically not in resonance with TAE.

3 NOVA TAE stability analysis

The NOVA-K hybrid code predicts $n = 10$ TAEs to be one of the most unstable in the nominal normal shear ITER plasma if both the alpha particle, γ_{α} , and beam ion, γ_{beam} , drives are combined [6]. The various damping mechanisms that significantly reduce the drive are ion Landau damping, γ_{iLand} , radiative damping, γ_{rad} , and trapped electron collisional damping, γ_{ecoll} , where γ is an imaginary part of TAE mode frequency, which describes the time evolution of the perturbed quantities $\exp(-i\omega t)$. Table 1 gives the growth and damping rates for the most unstable TAE in case of 0.55m off-axis NBI. Though the beams are at lower beta value

than the alpha particles, their drive is comparable due to their anisotropy at a fixed energetic particle energy density.

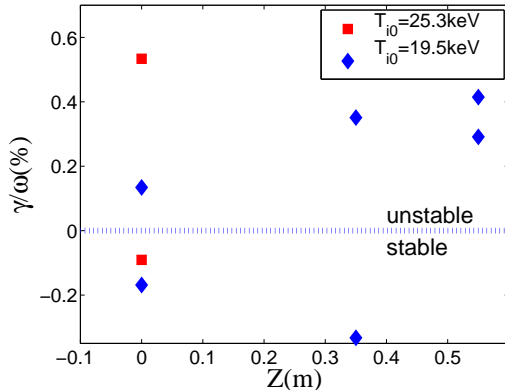


FIG. 3: Found $n = 10$ TAE growth rates as functions of NBI impact parameter ΔZ .

TAE instability. However even in that case, where $\beta_{\alpha 0} \simeq 1.33\%$, the pure fusion alpha-particle instability seems to still be marginally stable.

With NBI present, the instability drive is strong enough to cause instability, with the growth rates for the most unstable mode at $\gamma_{\Sigma}/\omega = 0.55\%$. Contribution to the drive from alphas or beam ions is typically 1–3% and as it is comparable to the damping rate the perturbative approach we use seems adequate. As the numerical results show most unstable TAEs are located in the Alfvén continuum gap with only a weak interaction with the continuum. At that point its amplitude is small which means that continuum damping is expected to be small [7, 8]. As the output of the TRANSP code shows, because of the neutral beam current drive, there is a low shear region at $0.4 < r/a < 0.6$ near the mode resonance with the Alfvén continuum, where $s < 0.3$. This implies that the “propagation” of TAE “couplets” into the center can be weak, with the result of low continuum damping $\gamma/\omega < 0.001$ [8].

Ω^2	$\gamma_{ecoll}/\omega(\%)$	$\gamma_{iLand}/\omega(\%)$	$\gamma_{rad}/\omega(\%)$	$\gamma_{\alpha}/\omega(\%)$	$\gamma_{beam}/\omega(\%)$	$\gamma_{\Sigma}/\omega(\%)$
0.96	-0.18	-0.61	-0.43	0.82	0.71	0.31

Table 1: Damping and driving growth rates of one of the most unstable $n = 10$ TAE.

4 Relaxation of fast ion profiles in multiple TAE unstable plasma

We attempt to answer a question whether there is likely to be a substantial loss of energetic particles due to diffusion from the fields generated by the TAE modes by applying a quasilinear diffusion model for alpha particle profiles.

In Ref. [6] the critical alpha particle pressure gradient was estimated from the balance between the energetic particle drive, the likely most important dissipative mechanisms arising from ion Landau damping and trapped electron collisions. Equating the drive to damping

The sum of damping and drive terms is plotted in figure 3 versus ΔZ_{NBI} , which is the vertical deviation from the magnetic axis of the beam injection line. The mode frequency is normalized according to $\Omega = \omega q_1 R_0 / v_{A0}$, where v_{A0} is the central Alfvén velocity, q_1 is the edge value of the safety factor. The more the beam is directed off-axis the stronger the drive is. This is because during the on-axis NBI, beam ion beta builds up near the plasma center, where the ion Landau damping is very strong. With the off-axis NBI the region of the strong beta gradient is shifted outward to the middle of the minor radius with strong drive and weak damping. At the higher ion temperature case, $T_{i0} = 25.3 \text{ keV}$, the fusion beta is larger which enhances alpha particle destabilization of the

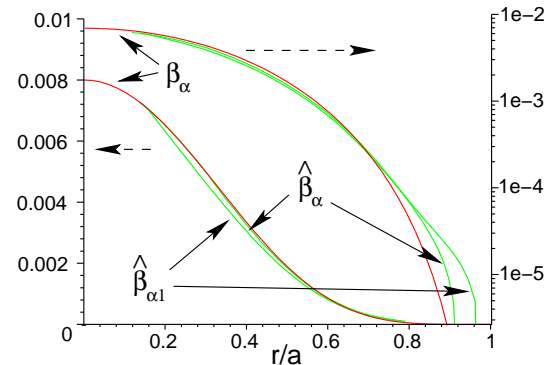


FIG. 4: Alpha particle beta profiles: initial, β_{α} , and reconstructed, $\hat{\beta}_{\alpha, \alpha 1}$, using the local critical beta from Eq.(5). Beta profile $\hat{\beta}_{\alpha 1}$ is obtained with the critical beta from Eq. (5) multiplied by 0.7. All the profiles are shown in linear and logarithmic scales.

terms gave,

$$\frac{\partial \beta_{\alpha cr}}{\partial r} = - \frac{\gamma_{iL} + \gamma_{ecoll}}{\gamma'_{\alpha}}, \quad (5)$$

where $\gamma_{\alpha}' = \gamma_{\alpha} / (\partial \beta_{\alpha} / \partial r)$, which is independent of the number of alphas. It was also shown that the two considered damping mechanisms are dominant for the expected radial location of the most unstable TAEs $r/a > 0.5$.

In this paper we show the results of the modeling and leave the discussion of the theory for a larger paper in progress. Fig. 4 shows results that have a benign effect on the alpha profile, unless the drive to damping ratio in Eq. (5) is boosted to $1/0.7$, which is denoted $\hat{\beta}_{\alpha 1}$ in the figure in which 4% losses of alphas are predicted. Stronger radial transport is predicted if the thermal ion temperature is raised as the fusion alpha-particle beta increases. Figure 5 shows the expected loss dependence with increased alpha particle beta as the temperature was increased from a baseline case $\beta_{pc0} = 6\%$, and $\beta_{\alpha 0} = 0.8\%$. We see that losses can become severe with increased temperature especially for the fixed beta case (note that MHD considerations may limit the operational beta to a fixed value).

5 Conclusions

We showed that NBI with tangential injection geometry are likely to destabilize TAEs in ITER-like plasma. Since the reactor plasma is supposed to be self-sustained without the beams, TAEs in a ITER-size machine is predicted to be marginally unstable. On the other hand NBI may provide an important tool for the experimental study of different types of AE instabilities by creating additional drive. Thus it is important to plan the NBI to be as flexible as possible in order to be able to change the conditions of AE excitation.

A quasi-linear model for alpha particle TAE induced transport based on the fast ion resonance overlap of the TAE modes efficiently evaluates the TAE driven transport and its effects on reactor performance. For the case studied it predicts the effect of TAEs will be tolerable over a band of ion temperature from about $20 - 23 keV$. However, the model is still in the process of development.

References

- [1] C. Z. Cheng, Phys. Reports, **211**, 1 (1992).
- [2] N. N. Gorelenkov, C. Z. Cheng, G. Y. Fu, Phys. Plasmas **7** 2802 (1999).
- [3] R. V. Budny, Nucl. Fusion **42** 1383 (2002).
- [4] H. L. Berk, W. Horton, M. N. Rosenbluth, and P. H. Rutherford, Nucl. Fusion **15**, 819 (1975).
- [5] C. Angioni, A. Pochelone, N. N. Gorelenkov, et.al, Plas.Phys.Contr.Fusion **44**, 205 (2002).
- [6] N. N. Gorelenkov, H. L. Berk, R.B. Budny, et. al. Nuclear Fusion **43**, 594 (2003).
- [7] H.L. Berk, J.W. Van Dam, Z. Guo, D.M. Lindberg, Phys. Fluids B **4** (1992) 1806.
- [8] M.N. Rosenbluth, H.L. Berk, J.W. Van Dam, D.M. Lindberg, Phys. Fluids B **4** (1992) 2189.

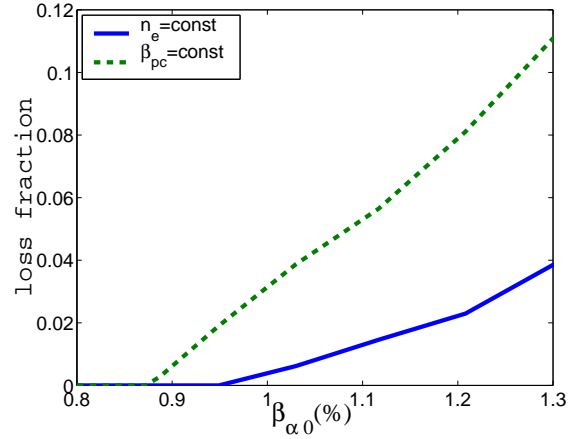


FIG. 5: Expected alpha particle losses are shown as function of increased $\beta_{\alpha 0}$ keeping fixed total plasma beta (dashed curve, $\beta_{pc} + \beta_{\alpha} = \text{const}$ in which $\beta_{\alpha 0} \sim T_{i0}^{5/2}$, $20 < T_{i0}(keV) < 24$) and density (solid curve, $\beta_{\alpha 0} \sim T_{i0}^{7/2}$, $20 < T_{i0}(keV) < 23$).